

Optical Design Study and Prototyping of a Dual-Field Zoom lens imaging in the 1-5 micron infrared waveband

Dmitry Reshidko*^a, Pavel Reshidko^b, Ran Carmeli^b

^aCollege of Optical Sciences, University of Arizona, Tucson, AZ, 85721, USA; ^bRP Optical Lab, 5 Shimshon St., Petah-Tikva, Israel 49517

ABSTRACT

Optical systems can provide simultaneous imaging in several spectral bands and thus be much more useful. A new and current generation of focal plane arrays is allowing detection in more than one spectral region. The design of a refractive imaging lens for such detectors requires correcting chromatic aberrations over the wider range of wavelengths. However, the fewer available refracting materials, the material properties that change between the spectral bands, and the system transmission requirements make the design of such lenses particularly challenging.

We present a dual-field zoom lens designed for a cooled detector sensing across short-wave infrared (SWIR) and mid-wave infrared (MWIR) spectral bands (continuous imaging for 1-5 μm). This zoom lens has a 75 mm focal length in the wide mode and a 250mm focal length in the narrow mode, and operates at f/4.7 in both discrete zoom positions. The lens is actively compensated to work in thermal environments from -20°C to $+60^{\circ}\text{C}$. We discuss the optical design methodology, review the selection of materials and coatings for the optical elements, and analyze the transmission of the lens and optical performance. A prototype system has been manufactured and assembled. We validate our design with experimental data.

Keywords: Zoom lens design, multi-band imaging, SWIR, MWIR

1. INTRODUCTION

Modern electro-optical systems for intelligence, surveillance and reconnaissance (ISR) applications are required to produce the highest quality images under a variety of different environmental conditions. Most systems feature zoom lenses along with additional system components such as laser designators and laser range finders, for example. Simultaneous imaging in several spectral bands is often required for efficient operation. The combination of short-wave infrared (SWIR, 1 to 2 μm) and mid-wave infrared (MWIR, 3 to 5 μm) detection bands is especially interesting since it enables the capability to perform active and passive imaging at the same time. Thermal imaging in the MWIR allows seeing in total darkness. The SWIR band provides daytime and low light level imaging and shows substantial advantage over visible light imaging (VIS, 0.4 to 0.7 μm) in the presence of atmospheric turbulence, haze, smoke and/or clouds. Furthermore, SWIR imaging adds the capability to detect laser rangefinder and designator frequencies.

Emerging cooled IR detectors enable the simultaneous imaging in both SWIR and/or MWIR spectral bands and onto the same focal plane. The size, weight and cost of a multiband imager with a single detector are considerably reduced by combining the optical path among the spectral bands. Furthermore, well-corrected optics designed for simultaneous imaging in multiple wavebands can solve possible image registration issues between bands. Calibration procedures to maintain boresight stability and repeatability of a zoom system can be substantially simplified, or avoided. The electrical power consumption of a multiband imager with a single detector is greatly reduced compared to a classic multi-sensor system.

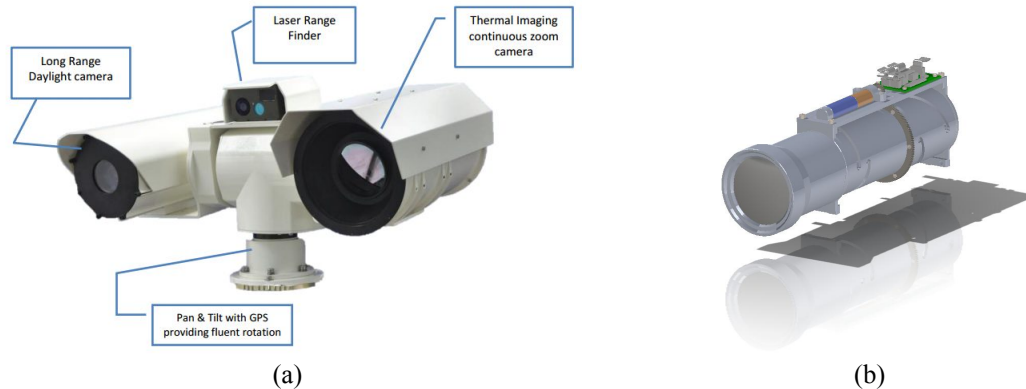


Figure 1. A multi-sensor system (a); a single aperture multi-band imager (b).

However, the complexity of the optical design task grows significantly with an increasingly wide spectral band. Conventional thought would dictate the implementation of a reflective-based system. But due to the system constraints discussed in Section 2, a refractive solution was deemed ideal. This leaves the optical designer with fewer refractive materials to choose from, material properties that change between the spectral bands, and with system transmission requirements, all of which make the design particularly challenging.

Lenses designed for operation in more than one spectral band have been reported in the past [1-8]. In this paper we present the optical design methodology for an all-refractive dual-field zoom lens imaging from $1\mu\text{m}$ to $5\mu\text{m}$ on the same focal plane. We concentrated on achieving a balanced performance over such wide spectral band while maintaining the manufacturability of the system, and keeping it compact and at a competitive cost. Optical solutions that require refocusing for operation in each spectral band or use complex mechanical mechanisms for interchangeable optical elements have not been considered in this study. We do not allow optical elements in the vacuum dewar of the cooled detector and do not take advantage of diffractive or GRIN optical elements to help aberration correction. Optical materials that have undesirable mechanical and chemical properties or poor transmission at the edge of the wavelength span are similarly not considered as a robust design is desirable.

2. SYSTEM SPECIFICATION

The lens design was performed with a cooled multi-function multi-band detector developed by Semi Conductor Devices (SCD), or similar multi-band detector, in mind [9]. This detector allows several modes of operation, imaging in both SWIR and MWIR bands simultaneously and detecting laser designator spots ($1.06\mu\text{m}/1.55\mu\text{m}$). The cold stop of the detector serves as the aperture stop of the system resulting in a fixed $f/4.7$ for both FOVs.

The dual-field-of-view system provides two discrete modes of operation: the wide-angle (short focal length) mode to observe the scenery and the narrow-angle (long focal length) mode to identify and classify the target of interest. The focal length of 250mm is often sufficient for recognition and identification of targets and provides a cost effective lens solution. For user convenience, the field-of-view zoom ratio is typically between 3-5:1[10]. The application requires a focusing range from 10-20m out to infinity. Thermal compensation from -20°C to $+60^{\circ}\text{C}$ is needed to allow operation under a variety of environmental conditions. Finally, it is desirable to keep the system more compact and lightweight compared to a traditional multi-sensor system.

The total system transmission is another major issue in the multi-band imager design. The correction of chromatic aberrations over the wide spectral band requires multiple optical elements. On the other hand, a coating efficient in both SWIR and MWIR bands is challenging to design and fabricate. Since the increased lens count can considerably decrease the overall system transmission, it is essential to keep the number of optical elements as low as possible.

Following the discussion above, a set of reasonable lens specifications is provided and summarized in Table 1.

Table 1. System specifications of the dual-field multi-band imager.

Parameter	Value
Focal Length	Dual FOV zoom lens – 75 & 250 mm
F#	4.7
Spectral Band	1-2 μm (Imaging) 3-5 μm (Imaging) 1.06/1.55 μm
Detector	SCD F/4.7 SNIR 640 x 512 x 15 μm
Total length	275mm
FFOV (diagonal)	Narrow 2.8° Wide 9.8°
Focus distance	25 m to Infinity – for Narrow 10 m to Infinity – for Wide
Transmissions	~80%
Operation temperature	-20°C to +60°C

3. REFRACTIVE DESIGN CONSIDERATIONS

The difficulty of this optical design comes mainly from the increased spectral band. In order to benefit from all unique capabilities of the multi-band detector, excellent correction of both monochromatic and chromatic aberrations over the entire FOV is required. Particularly, the correction of chromatic change of focus and chromatic change of magnification is essential in order to insure that the laser designator spot is on the target while still imaged in the MWIR. Moreover, it is also critical to reduce secondary and tertiary chromatic aberrations to obtain good image quality in each band individually.

The correction of chromatic aberrations in imaging systems is performed through the selection of optical glass. Methods for determining glass combination that reduce chromatic aberrations typically use aberration formulas or real raytracing. Aberration formulas, which are often based on the first order properties of the system, might be effective in some simple lenses or provides insight for initial material selection. The designs of two and three elements systems corrected for the extended spectral band has been discussed by other authors [1-4]. However, as the complexity of actual systems grows, simple metrics are not sufficient to estimate the final performance. For this reason, aberration correction is accomplished with real ray tracing. Although real ray tracing optimization is time demanding, it not limited to any specific bandwidth, can be used to correct chromatic and monochromatic aberrations to all orders, and support complex, multi-field-of-view systems. If the list of optical materials given to the program is relatively short, global optimization together with iterative substitution of similar glass types allows finding glass combinations and design configurations that are not otherwise obvious.

We reviewed the list of available optical materials that transmit in 1-5 μm wavelength range [1-4, 11-12]. We chose Schott's line of chalcogenide glasses over other similar chalcogenide glass types. Except BaF₂ and CaF₂, other Earth Alkali Halides have undesirable mechanical and chemical properties. Because of this, the other Earth Alkali Halides have been excluded from our available materials. Single point diamond-turned machining (SPDT) is the most practical option for fabricating optics from prototype to low production quantities. Materials that are not suitable or difficult for SPDT manufacturing, such as Sapphire or ALON, have not been considered. Finally, some materials, for example GaAs,

have poor transmission at the edge of the wavelength range and were excluded from the list. The plot of refractive index compared to wavelength range, as shown in Fig. 2, provides insight on the dispersive properties of the selected materials. For example, two optical materials are suitable for simultaneous correction over the wide spectral band, if both materials have the curve of refractive index versus wavelength similar in shape [1]. Unfortunately, there is no material pair that perfectly meets this requirement. IRG26 and IRG25/IRG24 is the closest match of materials. These two materials can be combined into doublets. IRG25/IRG24 have similar dispersive properties and can replace one another. We also notice that all selected materials, apart from BaF2 and CaF2, have larger dispersion in the SWIR comparing to the MWIR.

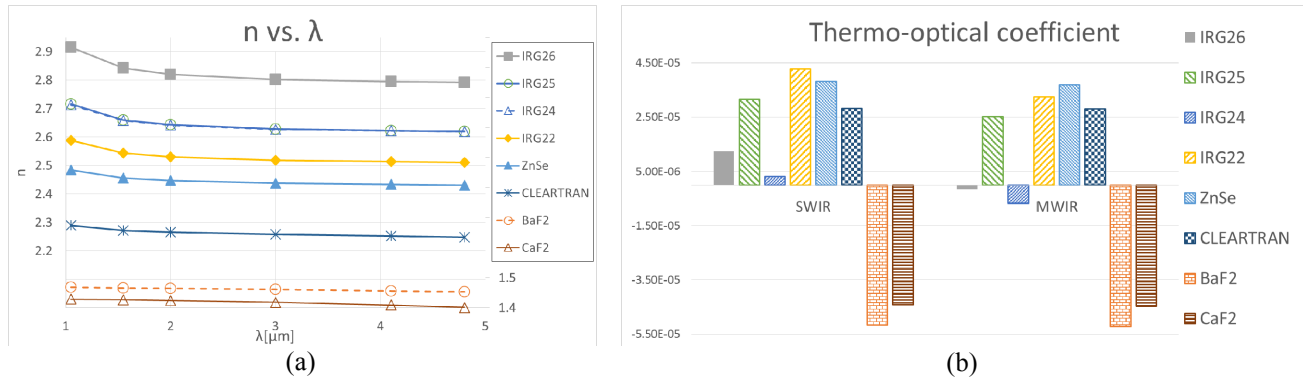


Figure 2. Materials that transmit in 1-5 μm wavelength range: (a) – dispersive properties; (b) – thermal properties.

A temperature change has the major effects of changing the index of refraction of the optical glass and geometry of the lens element. A first-order effect of a uniform temperature change in an optical system is to change the focal length. The thermo-optical coefficient characterizes how the focal length of a thin lens varies with temperature. The thermo-optical coefficient does not depend on the shape and size of the lens, but only on the physical and optical properties of the material. The thermo-optical coefficient, γ , can be calculated as,

$$\gamma = (dn / dT) / (n-1) - \alpha, \quad (1)$$

where α is the linear coefficient of thermal expansion and dn/dT is the thermal coefficient of refractive index. The change of focal length, Δf , due to a temperature change, ΔT , is given by

$$\frac{\Delta f}{f} = -\gamma \cdot \Delta T, \quad (2)$$

where f is the thin lens focal length. We calculate the thermo-optical coefficient for the selected materials for both SWIR and MWIR spectral bands. IRG26 and IRG24 have the lowest values of thermo-optical coefficient and relatively high refractive index. BaF2 and CaF2 are the only available materials with negative thermo-optical coefficient values.

Based on the information above, we further reduce the list of optical materials to the following: IRG26, IRG24, ZnSe, CLEARTRAN, BaF2 and CaF2.

4. OPTICAL DESIGN

The requirements for correction of both longitudinal and lateral chromatic aberrations, over the wide spectral band, impact the first order optical properties and configuration of the zoom lens. The FOV of the lens is changed by the axial movement of lens groups, which in turn affects the balance of aberrations within the system. We examine chromatic aberration contributions of each lens group. According to the Seidel theory, second order chromatic aberrations of a system of thin lenses can be calculated by tracing first-order marginal and chief rays.

$$\partial_{\lambda} W_{020} = \frac{1}{2} \sum_i \left[\frac{\phi}{v} y^2 \right] \quad (3)$$

$$\partial_{\lambda} W_{111} = \frac{1}{2} \sum_i \left[\frac{\phi}{\nu} y \bar{y} \right] \quad (4)$$

$$\Delta \partial_{\lambda} W_{020} = 0 \quad (5)$$

$$\Delta \partial_{\lambda} W_{111} = 2 \bar{S} \partial_{\lambda} W_{020} \quad (6)$$

In Eq. 3-6, y and \bar{y} are a marginal and chief ray height at lens i , ϕ is the power of lens i , ν is v-number and S is the stop shifting parameter. Between zoom positions, both object and pupil conjugates of the lens group change and the first order ray trace is altered. The chromatic change of focus is proportional to the marginal ray height and consequently depends on the object conjugates and on the pupil size. The chromatic change of magnification is proportional to both chief ray and marginal ray heights. As a result, the chromatic change of magnification depends on the pupil position as well. Eq. 5 and 6 show how chromatic aberrations change upon stop shifting. The chromatic change of focus is not affected by the stop shift. The chromatic change of magnification varies by the stop shift in the presence of the chromatic change of focus. Several different approaches for correcting chromatic aberrations in the zoom lens and achieving balanced performance for both FOVs have been investigated.

If each lens group is separately achromatized, it will remain achromatized in all zoom positions in spite of the pupil shift, changing pupil size and conjugates. However, achromatizing each group over the wide spectral band requires additional optical elements, which increase system cost and may reduce system transmission to unacceptable levels. Alternatively, one lens group can compensate for changing chromatic aberrations in the other group. In that case, it is desirable to minimize the variation in the chromatic aberration of each lens group during zooming.

The aperture stop of the system is located at the cold stop of the detector and is fixed in size. Therefore, the entrance pupil size increases with the focal length from the wide FOV to the narrow FOV to maintain a fixed $f/\#$. The magnitude of both chromatic change of focus and chromatic change of magnification will vary with the increasing pupil size. The correction of lateral chromatic aberrations in a lens with no symmetry around the aperture stop tends to be more difficult. If the pupil also shifts significantly during zooming it will be extremely hard to compensate for induced lateral color effects. Ideally, we want the optical configuration where pupil of each lens group maintains its position for both wide and narrow FOVs.

Once second order axial and lateral chromatic aberrations are corrected, then monochromatic and higher order chromatic aberration compensation is relatively easy. Since aspherical surfaces can be diamond turned without significantly increasing the cost of the optical element, we can take advantage of multiple aspherical lenses in our design to effectively correct residual aberrations. Notice that the beam footprint on the lens element changes between two FOVs and some aspherical surfaces can selectively correct aberrations in a single zoom position [13].

Optical design methodology

A three-lens group objective in a positive–negative–positive (P-N-P) power configuration has been widely used in the MWIR and LWIR zoom lens design [14]. The optically compensated continuous zoom lens requires at least two moving components: a negative zooming group and a positive focusing group. However, since only two fields-of-views are required, optical compensation can be achieved by the axial motion of a single lens group. The focusing group is fixed for two extreme magnifications. The zooming group operates at the reciprocal magnification, keeping the object and the image position stationary [10].

In order to clearly demonstrate the design procedure of the dual-field multi-band imager, we first present a relatively simple dual-field zoom lens imaging in the MWIR. System specifications of the lens, shown in Fig.3, are comparable to target specifications. In the design, a single lens moves for field-of-view switch, focus and thermal compensation. The system operates at $f/4$. The focal length in the narrow FOV is 250mm and the zoom ratio from the narrow field of view to the wide field of view is 5:1. The system consists of five aspherical lenses using Ge and Si as optical materials.

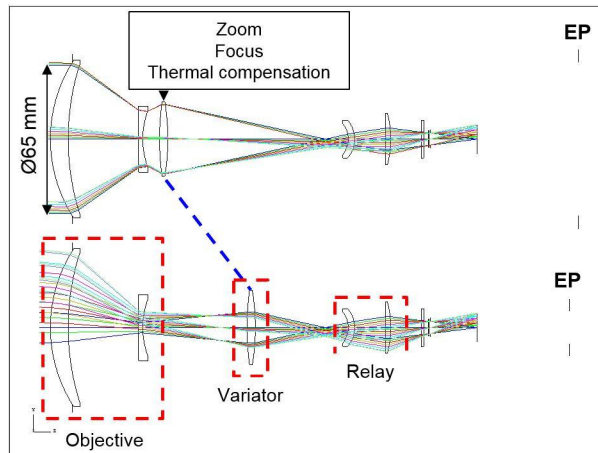


Figure 3. MWIR dual-field zoom lens used as a baseline design.

The design on Fig. 3 has diffraction limited image quality over the entire FOV range. Chromatic aberrations are well balanced without achromatizing each group separately. We analyze the first-order optical properties and the correction of chromatic aberrations in this dual-field zoom lens.

The front lens is usually the largest and the most expensive optical element. The aperture stop position at the cold stop may cause pupil wander on the objective lens. Adding reimaging optics allows efficiently controlling the beam footprint and minimizing the lens diameter. Usually the entrance pupil in the narrow FOV is placed close to the front element. In this design, on the other hand, the pupil reimaging scheme is different and is used to both minimize the variation of chromatic aberrations between two zoom positions and control the front lens size. The aperture stop of the system is at the cold stop of the detector. The relay lens group is fixed and its chromatic aberrations do not change during zooming. The relay optics is reimaging the aperture stop close to the moving element. As the result, the variator group contributes a small amount of chromatic change of magnification since the chief ray height on the lens is small in both configurations. The objective lens group is used with relay optics to fix the entrance pupil position for both FOVs. The entrance pupil position is chosen to balance the lateral chromatic aberration contribution of the objective group. The increasing marginal ray height in the narrow FOV is compensated by the increasing chief ray height in the wide FOV and the objective group contributes the same amount of chromatic change of magnification in both configurations. The front lens diameter is only 2mm larger than the entrance pupil diameter in the narrow FOV and is controlled by introducing small amount of pupil spherical aberration.

Another critical component of this design is a field lens positioned close to the intermediate image plane. The field lens helps flattening the field by introducing astigmatism and field curvature. Moreover, Dialyte type designs often leave a huge amount of uncorrected lateral color. The field lens is controlling the heights of the chief rays of different colors at the relay lens allowing compensating both longitudinal and lateral chromatic aberrations induced in the front group [15-17].

Second order chromatic aberration contributions of each lens group are calculated using Eq. 3-4 and shown in Fig. 4. Notice that each group contributes similar amount of chromatic change of magnification in both configurations. Contributions to the chromatic change of focus scale with the increasing pupil size. Small residual chromatic aberration is almost identical in both configurations and can be removed with a single diffractive surface on the back side of the last lens. Chromatic aberrations are compensated without achromatizing each group separately.

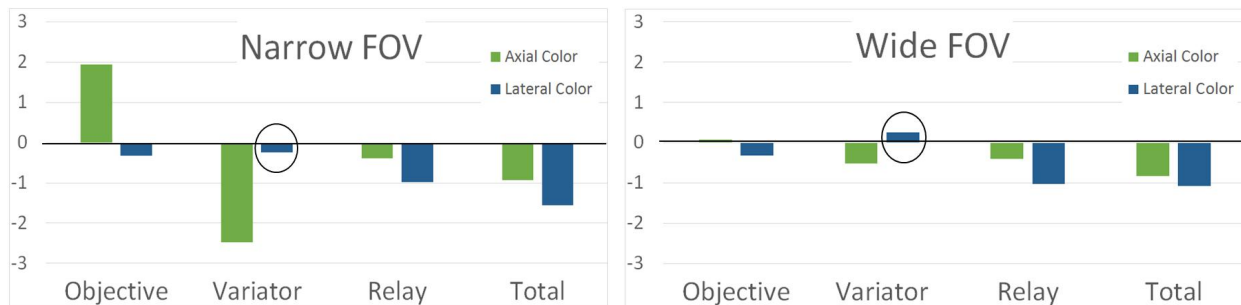


Figure 4. Second order chromatic aberrations of the MWIR dual-field zoom lens.

Optical design with single moving group

A similar approach was used to design a dual-field lens for the 1-5 μm spectral band. We started with the monochromatic design and configuration in Fig. 3. Each group was separately achromatized for the wide spectral band. Complete system optimization allowed each group to depart from this condition. Through optimization, it was possible to remove several lenses. The system layout is shown in Fig. 5.

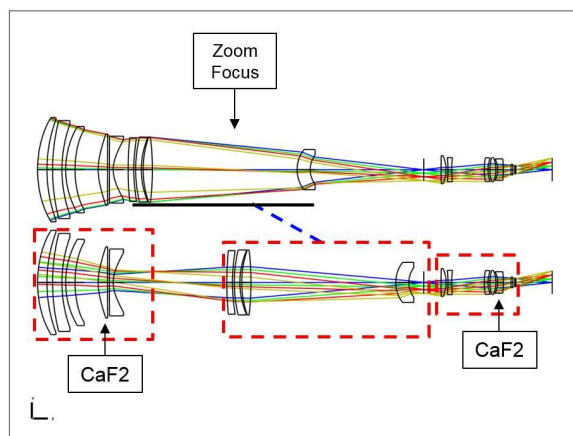


Figure 5. Wide spectral band dual-field zoom lens with a single moving group (Option I).

The optical path difference (OPD) fans for wide and narrow FOVs are presented in Fig. 6. Although the lens shows excellent correction of both chromatic and monochromatic aberrations, fourteen optical elements were used in this design. Reduction of optical elements was critical to achieve the transmission requirements. The materials used were ZnSe, CLEARTRAN, IRG24, IRG26 and CaF₂. As before, a single lens group was used for zooming and focusing. A change from the baseline design showed that thermal compensation required moving components in the relay group.

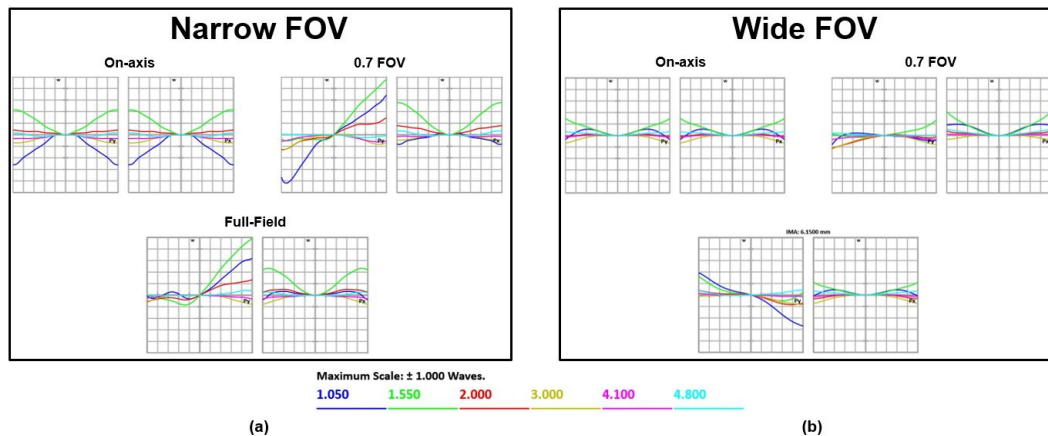


Figure 6. OPD fans for both narrow FOV (a) and wide FOV (b). Although the lens shows excellent optical performance, fourteen elements were used in this design.

Optical design with two moving groups

In order to meeting the lens transmission specification and keep the design at competitive cost, we needed to further reduce the number of optical elements. To achieve the element reduction, a slightly different zooming mechanism was utilized which still minimized the pupil shift.

In the previous section, we showed that a single moving group was not sufficient to meet the design specification. We allowed lenses in the relay group to move during zooming. Following extensive optimization, a design was reached which provided an excellent level of optical performance. The final optical system is composed of a positive overcorrected front group and a positive undercorrected relay group. The front group consists of two static widely spaced positive doublets and two additional widely spaced doublets, positive and negative, which move together during zooming. The relay group consists of a static singlet and a field lens positioned close to the intermediate image plane. The field lens position is adjusted during zooming. Both moving groups act as variators. Focus and thermal compensation is accomplished by the displacement of the field lens. The final system layout is shown in Fig. 7

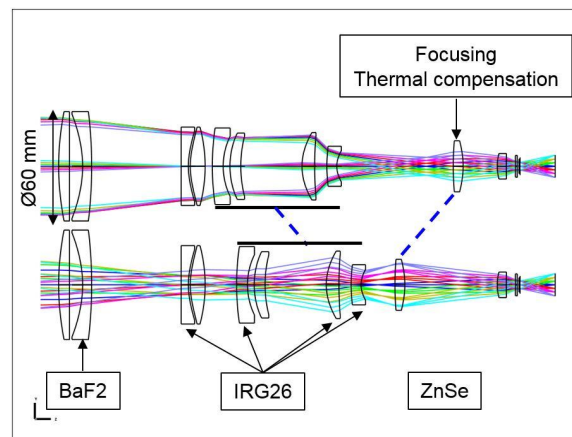


Figure. 7 Wide spectral band dual-field zoom lens with two moving groups (Option II).

Excellent aberration correction over the wide spectral band is achieved for both FOVs using only ten aspherical elements and three optical materials. The materials are ZnSe, IRG26 and BaF2. The OPD fans of the final design are shown in Fig. 8. The optical path difference for the on axis field point is less than 0.2 waves: chromatic change of focus, spherical aberration and spherochromatism are well balanced in both configurations. The off-axis performance degrades mainly due to lateral color at SWIR wavelengths.

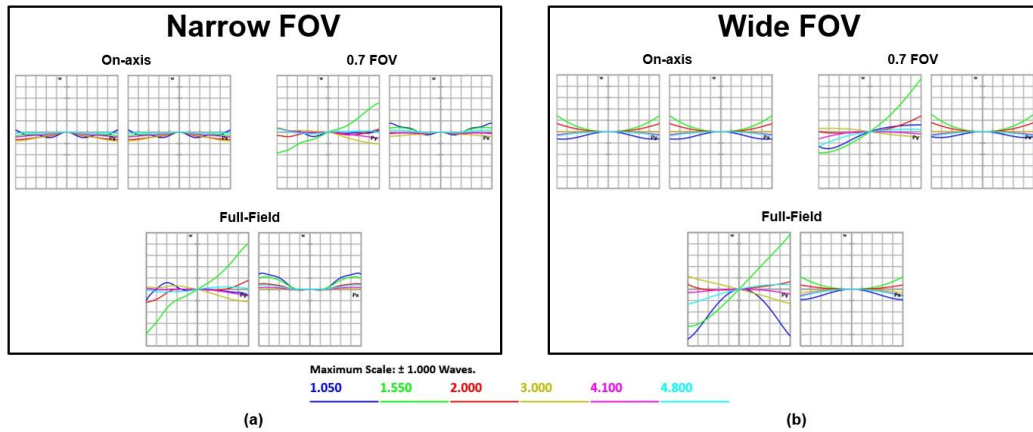


Figure 8. OPD fans of the final design for both narrow FOV (a) and wide FOV (b) show excellent correction of chromatic and monochromatic aberrations.

5. FINAL PERFORMANCE

In this section, we evaluate the optical performance of the final design. We discuss nominal image quality in each operation mode, analyze the effect of temperature change and manufacturing tolerances on the final performance, present coatings developed for this broadband system and estimate the total transmission of the lens.

Image quality

The polychromatic MTF for the SWIR band, MWIR band, and combined imaging in the SWIR/MWIR bands are shown in Fig. 9-11. The MTF was calculated for 1.06 μm , 1.55 μm and 2 μm in the SWIR, and 3 μm , 4.1 μm and 4.8 μm in the MWIR equally weighted over the spectrum. The MTF plots are evaluated at the same focal plane. Both the MWIR-only and SWIR-only MTF is close to being diffraction limited over about 60% of the FOV. The performance degrades slightly toward the edge of the field in the MWIR-only system. Sagittal MTF at high frequencies for the SWIR-only system varies significantly with the increasing field angle, but overall image quality at the detector corners is still reasonable. The combined SWIR/MWIR MTF is a spectral average of the single band MTF. The nominal system image quality is predominantly acceptable over the wide spectral band.

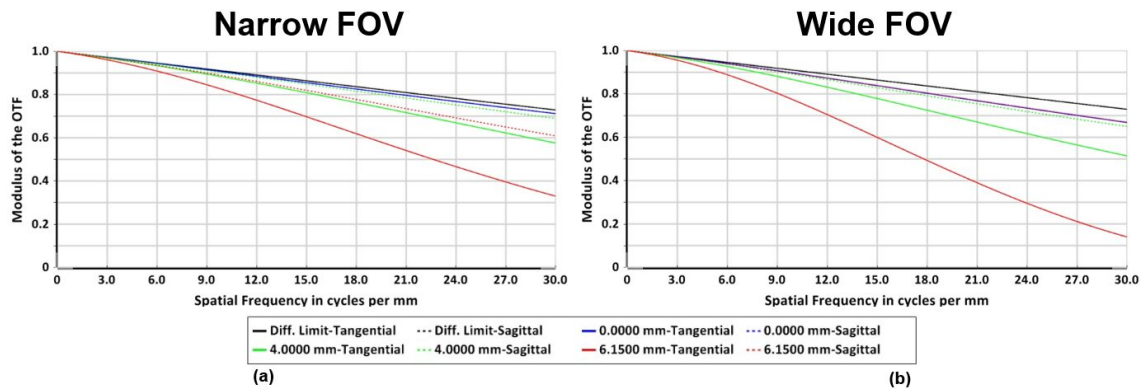


Figure 9. Polychromatic MTF in the SWIR for narrow FOV (a) and wide FOV (b).

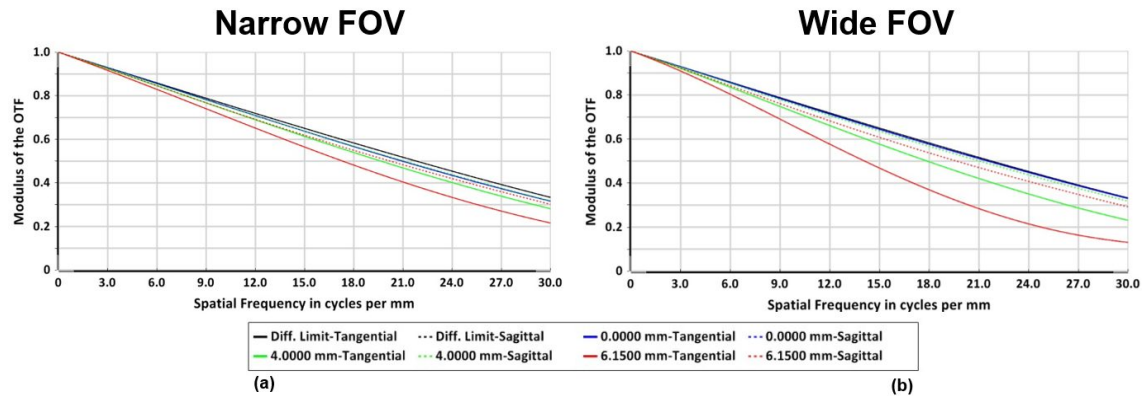


Figure 10. Polychromatic MTF in the MWIR for narrow FOV (a) and wide FOV (b).

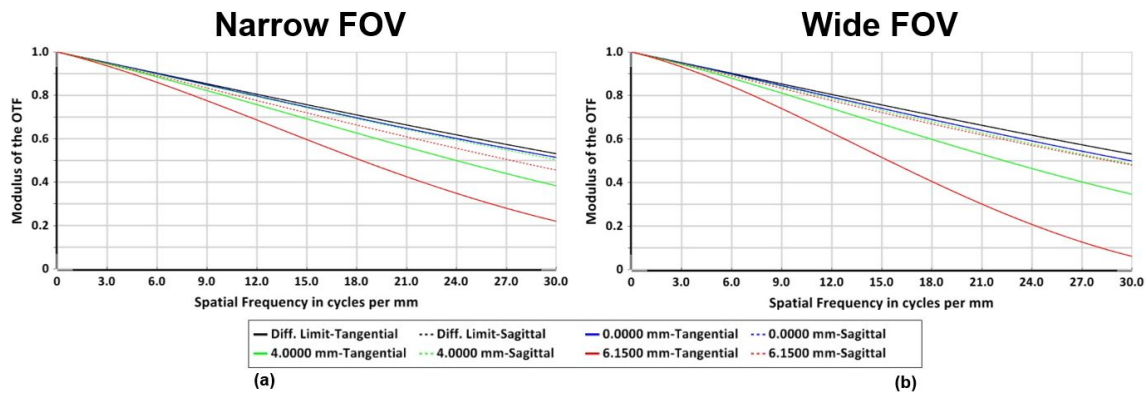


Figure 11. Polychromatic MTF in the SWIR/MWIR for narrow FOV (a) and wide FOV (b).

Thermal compensation

The thermal stability is another key requirement for the zoom lens. In a lens system, a temperature change has the effect of changing the index of refraction and the geometry of the optical elements. Therefore, first-order imaging properties and aberration balance of the nominal design are affected and it may fail to maintain the desirable image quality over the whole range of possible temperatures.

The nominal system satisfies both monochromatic and chromatic aberration correction requirements at +20°C. The effect of the uniform temperature change for the temperature range from -20°C to +60°C was simulated. The thermal coefficient of refractive index, dn/dT , characterizes how the index of refraction of the material varies with the temperature. However, the thermal coefficient of refractive index depends on the wavelength and varies significantly from SWIR to MWIR spectral bands. A single parameter is not sufficient to accurately model the variation of the index of refraction for the wide spectral band. We used actual values of the index of refraction of ZnSe, IRG26 and BaF2 found in related scientific papers to fit a glass dispersion formula at each temperature.

The field lens in the relay group is used for active thermal compensation [18]. OPD fans for the on-axis and full field points at -20°C, +20°C and +60°C are shown in Fig. 12. The aberration correction remains well balanced over the required temperature range. Less than two waves of axial and lateral color are induced at the shorter SWIR wavelength.

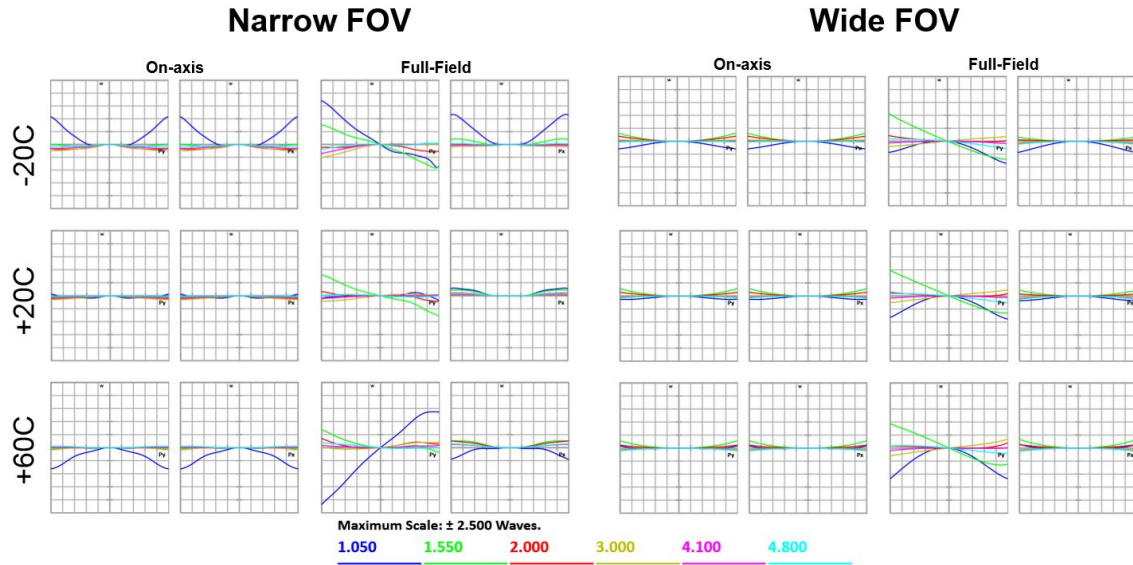


Figure 12. The effect of the uniform temperature change on the optical performance. The aberration correction remains well balanced over the required temperature range.

Tolerance analysis

It is important to provide insight on the sensitivity to manufacturing tolerances and estimate the as-built performance of the zoom lens. The main disadvantage of the presented design is large amounts of aberrations propagating in the system and, as a result, increased sensitivity to misalignments. Comprehensive tolerance analysis of the lens has been carried out. A tolerance budget for optics and opto-mechanics has been estimated, while not presented here. Although, as expected, some tolerance values are relatively tight, the final set of tolerances is readily achievable with the SPDT lens manufacturing and standard assembly and alignment procedures.

Aggregate effects of all tolerances have been estimated with a Monte Carlo simulation. We considered a worst-case scenario and use minimum MTF across the field as a criterion. We analyze sixteen field points as shown in Fig.13 . We ran three separate simulations for 60%, 80% and 100% of the FOV. The compensators for this system are the decenter of the front doublet and the back focus position.

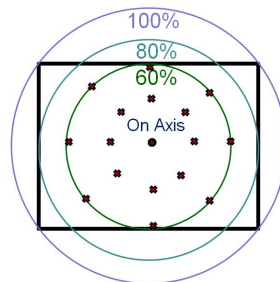


Figure 13. Visualization of the Monte Carlo criterion

Fig. 14 shows the cumulative probability distributions for the minimum MTF for the wide and narrow FOVs. The horizontal axis corresponds to the minimum MTF value while the vertical axis gives the probability achieving that MTF value or better. Zero probability provides the nominal design values and the 100% probability level indicates the guaranteed minimum MTF in any assembled system.

In the wide FOV each probability curve climbs sharply to the 90% level: no significant lost in the image quality is expected in the assembled system. The on-axis as-built performance in the narrow FOV is anticipated to be close to the

nominal design as well. Although the image may appear blurry in the corners of the detector in the narrow FOV, decent performance is preserved for at least 60% FOV.

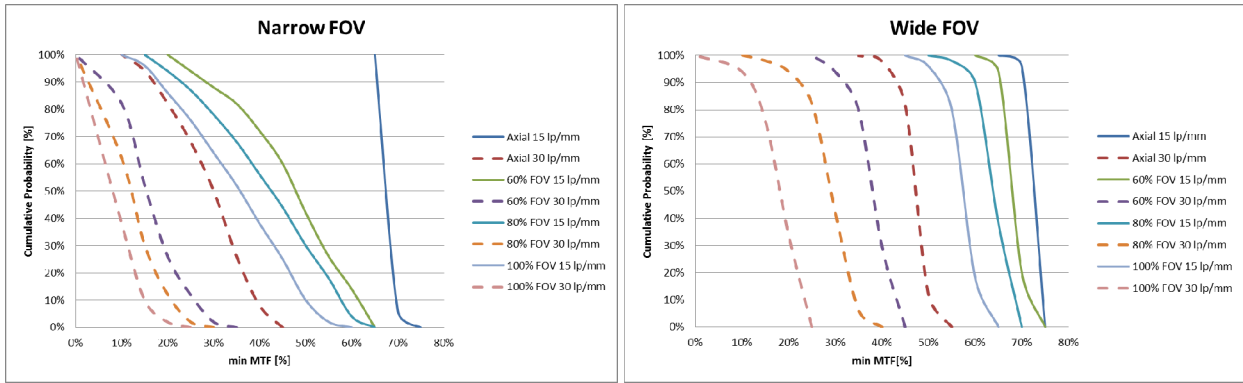


Figure 14. Monte Carlo Tolerancing Probability for minimum Polychromatic MTF across the field.

Coating and transmission

Application of anti-reflection coatings significantly reduces Fresnel reflections and improves the transmission of the lens. A coating efficient in both SWIR and MWIR bands is challenging to design and fabricate. Special wide spectral-band anti-reflection coatings for ZnSe, IRG26 and BaF₂ were developed for this application [19]. A single surface reflection curve for normal incidence is plotted in Fig. 15a. The coatings were optimized for the best performance in the MWIR and at the laser designator wavelengths (1.06 μ m/1.55 μ m). Although the transmission drops considerably in 2-3 μ m region, the system performance in this wavelengths range is less critical due to increased atmospheric absorption. Full system throughput is shown in Fig.15b. The total transmission has been estimated by calculating surface losses and material absorption for a ray traced along the optical axis to be more than 80% in the MWIR and at the laser designator wavelengths.

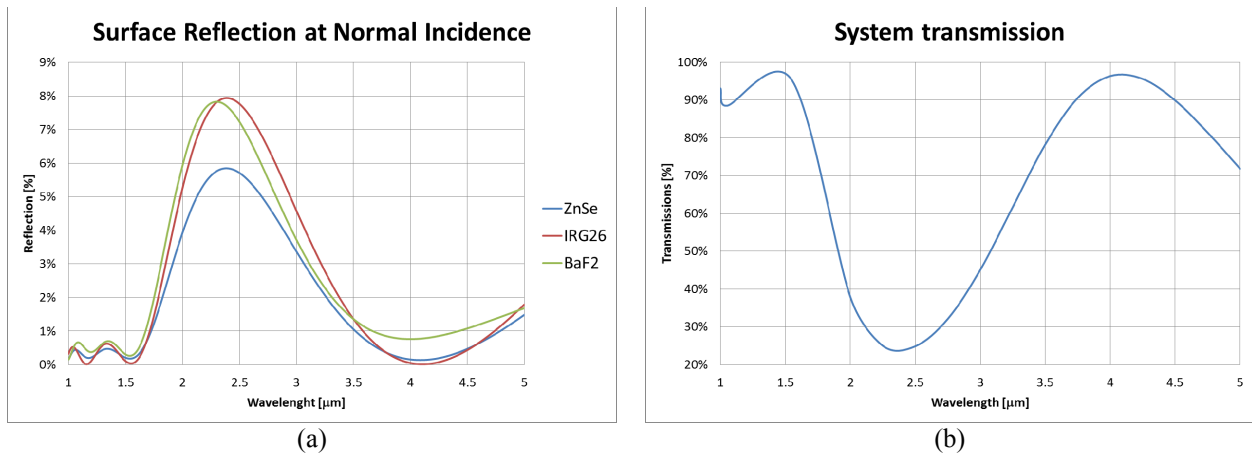


Figure 14. Wide spectral band anti-reflection coatings and estimated system transmission.

6. PROTOTYPE

A prototype system has been manufactured, assembled and tested. A photograph of the lens is shown in Fig.15. The actual multi-band detector was not available at the time and preliminary images were collected with two single band detectors. Wide FOV imagery for the SWIR and MWIR bands is shown in Fig. 16a and Fig. 16b. Resolution of the lens in the Narrow FOV was validated by imaging a test chart. Bar targets corresponding to 22-25 lp/mm display reasonable contrast and are presented in Fig. 16c and Fig. 16d.

Future work will explore designs of a continuous zoom system as well as evaluating this system performance in all operation modes with the actual detector.

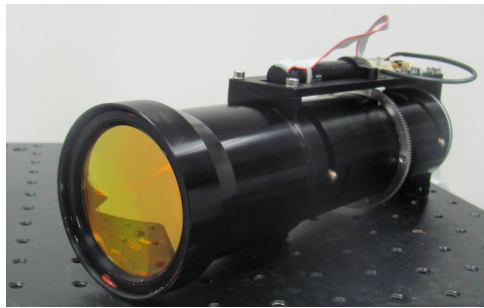


Fig. 15. Assembled prototype of the dual-field multi-band imager

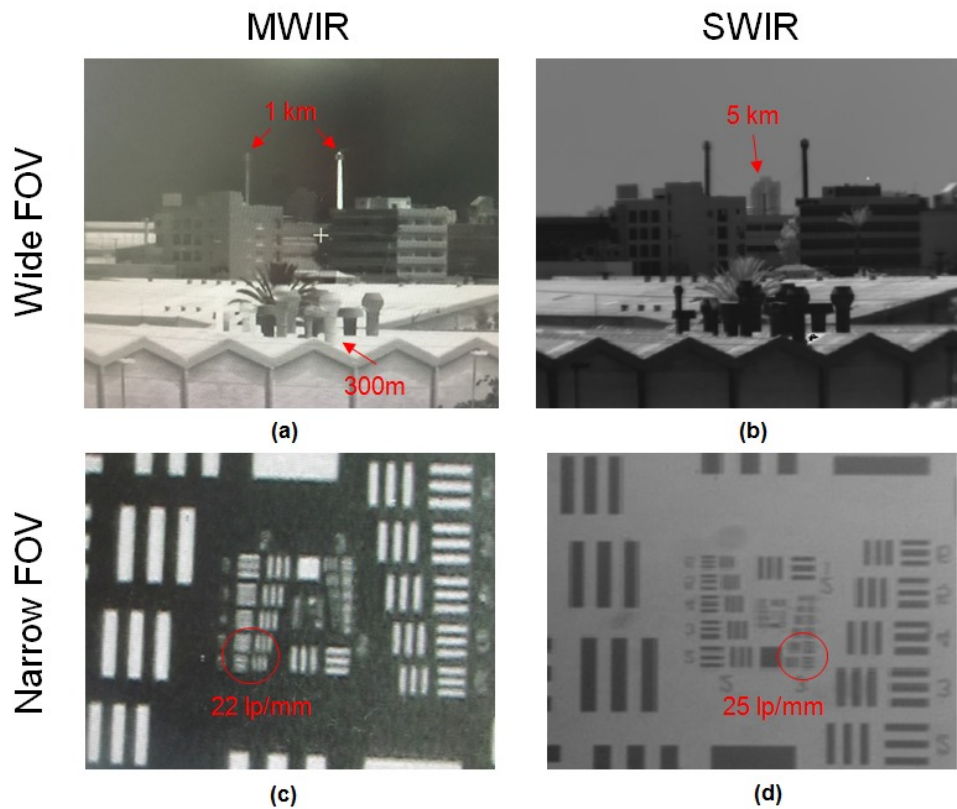


Fig. 16. Wide FOV imagery for the SWIR (a) and MWIR (b). Resolution chart in the Narrow FOV: MWIR (c) and SWIR (d).

7. CONCLUSION

We outlined the design process of an all-refractive dual-field zoom lens imaging in the $1\mu\text{m}$ to $5\mu\text{m}$ wavelength range and on the same focal plane. Because of the increased spectral band, the lens design process produced some interesting solutions. In this paper, we emphasized the high image quality, manufacturability, compact packaging, and the relation to overall system cost.

The final solution utilizes ten aspherical optical elements and meets image quality requirements in all operation modes. We demonstrated that it is possible to correct chromatic aberrations over the wide spectral band using only three optical material – ZnSe, IRG26 and BaF₂. Reducing the materials count provides an advantage in lens manufacturing and in the

antireflection coating of the lens surfaces. We showed wide spectral band anti-reflection coatings that were developed for this application and estimated the average system transmission at 1.06 μ m/1.55 μ m/MWIR to be approximately 80%. The system performance is limited by the transmission that drops considerably in the 2-3 μ m region. Different coatings can be applied for operation anywhere in the 1 μ m to 5 μ m range. Even with these considerations, the lens provides excellent imaging over the full 1-5 μ m waveband.

The requirements for correction of both longitudinal and lateral chromatic aberrations over the wide spectral band affect the first order optical properties and configuration of the zoom lens. We discussed the methodology for achieving two FOVs and compensating chromatic aberration in the zoom lens without achromatizing each lens group separately. Two moving groups are used in the final design. The movement of both groups is implemented with a single driving motor.

The effect of manufacturing tolerances and thermal environment on the optical performance of the lens has been analyzed. We concluded that no significant loss in the image quality is expected in the assembled system and that the aberration correction remains well balanced over the required temperature range.

Finally, a prototype system has been manufactured and assembled. We validated our design with experimental data.

ACKNOWLEDGMENTS

The authors wish to acknowledge Eric Herman at The Aerospace Corporation and Prof. Jose Sasian at the University of Arizona for their time in assisting in reviewing this paper.

REFERENCES

- [1] T. H. Jamieson, "Ultrawide waveband optics," *Opt. Eng.* 23(2), 232111 (1984)
- [2] M. P. Snyder, J. N. Vizgaitis, "Optical design study for the 1-5 μ m spectral band," *Proc. SPIE* 7298 (2009)
- [3] P. McCarthy, et.al., "Optical Design Study in the 1-5 μ m Spectral Band with Gradient-Index Materials," *Proc. SPIE* 9293 (2014)
- [4] E. Herman, et.al., "System design process for refractive simultaneous short and long wave infrared imaging," *Appl. Opt.* 52, 2761-2772 (2013)
- [5] B. E. Catanzaro, et.al., "Design of dual-band SWIR/MWIR and MWIR/LWIR imagers," *Proc. SPIE* 5406 (2004)
- [6] H. M. Spencer, "Optical Design Considerations for Wide Spectral Band Applications using Refractive Optics," *Proc. SPIE* 9293 (2014)
- [7] S. Lilley, et. al., "Multifield of view see-spot optics," *Opt. Eng.* 52(6) (2013)
- [8] J. Vizgaitis, "Third generation infrared optics," *Proc. SPIE* 6940 (2008)
- [9] L. Langof, et. al., "Advanced multi-function infrared detector with on-chip processing," *Proc. SPIE* 8012 (2011)
- [10] R. E. Aldrich, "Three-element infrared optically compensated two-position zooms for commercial FLIRs," *Proc. SPIE* 2539 (1995)
- [11] H. H. Li, "Refractive index of ZnS, ZnSe, and ZnTe and its wavelength and temperature derivatives," *J. Phys. Chem. Ref. Data*, Vol. 13, No. 1 (1984)
- [12] H. H. Li, "Refractive index of Alkaline Earth Halides and its wavelength and temperature derivatives," *J. Phys. Chem. Ref. Data*, Vol. 9, No. 1 (1980)
- [13] E. I. Betensky, "Role of aspherics in zoom lens design," *Proc. SPIE* 1354 (1991)
- [14] A. Mann, "Infrared Optics and Zoom lenses," *SPIE Press* (2009)
- [15] R. Blakley, "Dialyte-refractor design for self-correcting lateral color," *Opt. Eng.* 42(2) (2003)
- [16] R. Duplov, "Achromatic telescope without anomalous dispersion glasses," *Appl. Opt.* 45 (2006)
- [17] M. R. Aguilar, "Application of the extended first-order chromatic theory to the correction of secondary spectrum," *Revista Mexicana de Física* 43 (1997)
- [18] E. H. Ford, "Active temperature compensation of an infrared zoom lens," *Proc. SPIE* 3129 (1997)
- [19] ISP Optics Corporation, Ltd